3-1-2009

Online Synchronous Machine Parameter Extraction from Small-Signal Injection Techniques

Jing Huang

Keith Corzine
Missouri University of Science and Technology

M. Belkhayat

Recommended Citation

J. Huang et al., "Online Synchronous Machine Parameter Extraction from Small-Signal Injection Techniques," *IEEE Transactions on Energy Conversion*, Institute of Electrical and Electronics Engineers (IEEE), Mar 2009.
The definitive version is available at https://doi.org/10.1109/TEC.2008.2008953

Online Synchronous Machine Parameter Extraction From Small-Signal Injection Techniques

Jing Huang, *Student Member, IEEE*, Keith A. Corzine, *Senior Member, IEEE*, and Mohamed Belkhayat

***Abstract*—This paper proposes using a novel line-to-line voltage perturbation as a technique for online measurement of synchronous machine parameters. The perturbation is created by a chopper circuit connected between two phases of the machine. Using this method, it is possible to obtain the full set of four complex small-signal impedances of the synchronous machine d–q model over a wide frequency range. Typically, two chopper switching frequencies are needed to obtain one data point. However, it is shown herein that, due to the symmetry of the machine equations, only one chopper switching frequency is needed to obtain the information. A 3.7-kW machine system is simulated, and then constructed for validation of the impedance measurement technique. A genetic algorithm is then used to obtain IEEE standard model parameters from the d–q impedances. The resulting parameters are shown to be similar to those obtained by a series of tests involving synchronous reactance measurements and a standstill frequency response.**

***Index Terms*—Generator, genetic algorithm (GA), impedance, motor, online measurement, parameter, synchronous machine.**

I. Introduction

THE IDENTIFICATION of synchronous machine parameters is necessary for analysis of performance and control of synchronous machines. For applications such as systems with power electronic loads having high bandwidth regulation, stability becomes very critical, and appropriate system models with accurate machine parameters will be necessary for stability prediction. In other applications, harmonic requirements, such as recommended by IEEE 519 and practiced by industry standards, are becoming stricter. Predicting current and voltage harmonics at the machine terminals necessitates accurate machine parameters, which would reflect operating conditions as closely as possible. In yet other applications, tracking key machine parameters versus time for the life of the machine can be used for condition monitoring. Given the appropriate parameters, condition monitoring can be used not only for sudden failure prevention but also for lowering the entire life-cycle cost. Finally, accurate parameters that reflect realistic operating conditions or that are updated over the life of the machine are more useful for model-based control than parameters that are measured only once or derived from static tests.

In the past decades, many methods have been developed to identify parameters of synchronous machines that can generally be grouped into two categories: standstill measurement and online measurement. The standstill frequency response (SSFR) test is applied when the machine is stationary [1]. Although SSFR tests are very useful for machine parameter extraction, they do not represent the synchronous machine characteristics accurately under normal operating conditions. For example, the effect of three-phase rated currents on the magnetic operating point is not considered. For an accurate harmonic analysis at the machines terminals, consideration of these effects is desirable. Thus, a need for identification of synchronous machine parameters under real operating conditions arises.

Many online synchronous machine parameter identification procedures [2]–[8] have gained attention recently. Some of these methods rely on large disturbance response, such as load rejection. Some tests need measurement of the machine in q- and d-axis separately, which has some difficulty in practice. Several multistage machine parameter identification methods were proposed in [5]–[8], which used small excitation disturbance data and a variety of estimation techniques to extract the parameters.

A method of parameter measurement is presented in [9] where the synchronous machine electrical characteristics are identified in the frequency domain by running the machine at different speeds. The method adopts a line-to-line short circuit between two terminal phases and small excitation of the field to obtain operating rather than standstill conditions. The method presented herein differs in that the small-signal parameters are obtained during rated, balanced operation.

In this paper, a new online approach is proposed that is based on a small-signal injection between two phases using a power electronic chopper circuit to measure d–q impedance of the synchronous machine. The injected current is around 5% of the rated stator current, a value high enough to obtain an impedance measurement, but low enough not to disturb normal operation. Also, a d–q impedance matrix is derived with both d- and q-axis information so that there is no need to do a test on each axis separately. The d–q impedance matrix related to the machine parameters does not impose any limitations on the number of damper windings, so more accurate models can be used when needed, especially in the case of solid iron rotor machines.

The method proposed in this paper allows measuring the synchronous machine parameters when the machine is under rated operating condition. The key component, a chopper circuit, is very simple to construct and can be applied to median voltage systems.

This paper begins with a derivation of the d–q impedance of a synchronous machine. Next, the technique of small-signal injection and practical implementation is set forth. Once the

Manuscript received November 12, 2007; revised June 28, 2008. Current version published February 19, 2009. Distribution Statement A: Approved for Public Release, distribution is unlimited. Paper no. TEC-00427-2007.

J. Huang and K. A. Corzine are with the Department of Electrical and Computer Engineering, Missouri University of Science and Technology, Rolla, MO 65409-0040 USA (e-mail: corzinek@mst.edu).

M. Belkhayat is with Northrop Grumman Newport News, Washington, DC 20003 USA.

Digital Object Identifier 10.1109/TEC.2008.2008953

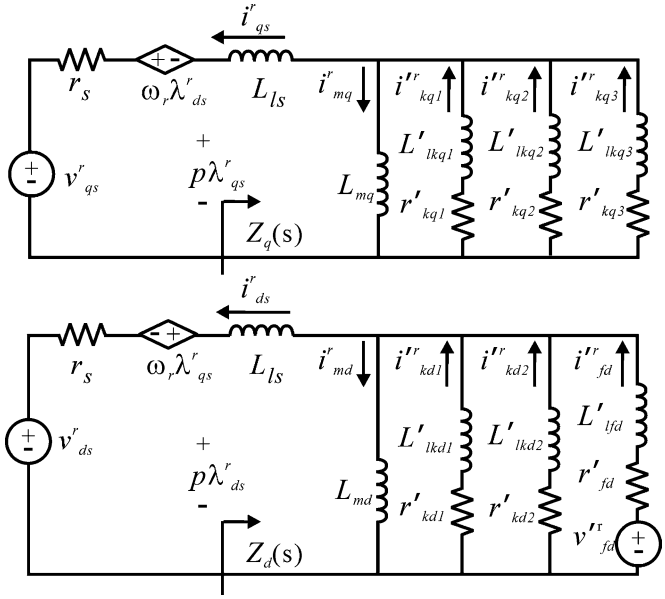

Fig. 1. Equivalent d–q circuits of a synchronous machine.

d–q impedance matrix is determined, a genetic algorithm (GA) is applied to estimate the parameters. Simulation and a laboratory tests verify the proposed method.

II. Synchronous Machine Model

Herein, the electrical model of the synchronous machine is chosen based on the IEEE standard 1110 [10] in which two damper windings on the d-axis and three damper windings on the q-axis are modeled to portray adequately the transient characteristics of a synchronous machine. The equivalent circuits of this model are shown in Fig. 1. Herein, the direction of positive stator current is out of the terminals, as shown in Fig. 1. Using this convention, the voltage equations of synchronous machine may be expressed in the rotor synchronous frame as [11]

$$\begin{bmatrix} v^r_{qs} \\ v^r_{ds} \\ v'^r_{kqx} \\ v'^r_{kdy} \\ v'^r_{fd} \end{bmatrix} = \begin{bmatrix} -r_s & 0 & 0 & 0 & 0 \\ 0 & -r_s & 0 & 0 & 0 \\ 0 & 0 & r'_{kqx} & 0 & 0 \\ 0 & 0 & 0 & r'_{kdy} & 0 \\ 0 & 0 & 0 & 0 & r'_{fd} \end{bmatrix} \begin{bmatrix} i^r_{qs} \\ i^r_{ds} \\ i'^r_{kqx} \\ i'^r_{kdy} \\ i'^r_{fd} \end{bmatrix} + \begin{bmatrix} \omega_r & 0 \\ 0 & -\omega_r \\ 0 & 0 \\ 0 & 0 \\ 0 & 0 \end{bmatrix} \begin{bmatrix} \lambda^r_{ds} \\ \lambda^r_{qs} \end{bmatrix} + \begin{bmatrix} 1 & 0 & 0 & 0 & 0 \\ 0 & 1 & 0 & 0 & 0 \\ 0 & 0 & 1 & 0 & 0 \\ 0 & 0 & 0 & 1 & 0 \\ 0 & 0 & 0 & 0 & 1 \end{bmatrix} \begin{bmatrix} p\lambda^r_{qs} \\ p\lambda^r_{ds} \\ p\lambda'^r_{kqx} \\ p\lambda'^r_{kdy} \\ p\lambda'^r_{fd} \end{bmatrix} \tag{1}$$

where ω_r is the speed of the rotor reference frame, x represents the number of damper windings on the q-axis, which can be 1, 2, or 3, and y represents the number of dumper on the d-axis, which can be 1 or 2. The rotor variables are referred to the stator windings for convenience. The flux linkages may be written as [11]

$$\begin{bmatrix} \lambda^r_{qs} \\ \lambda^r_{ds} \\ \lambda'^r_{kqx} \\ \lambda'^r_{kdy} \\ \lambda'^r_{fd} \end{bmatrix} = \begin{bmatrix} -L_{ls} & 0 & 0 & 0 & 0 \\ 0 & -L_{ls} & 0 & 0 & 0 \\ 0 & 0 & L'_{lkqx} & 0 & 0 \\ 0 & 0 & 0 & L'_{lkdy} & 0 \\ 0 & 0 & 0 & 0 & L'_{lfd} \end{bmatrix} \begin{bmatrix} i^r_{qs} \\ i^r_{ds} \\ i'^r_{kqx} \\ i'^r_{kdy} \\ i'^r_{fd} \end{bmatrix} + \begin{bmatrix} L_{mq} & 0 \\ 0 & L_{md} \\ L_{mq} & 0 \\ 0 & L_{md} \\ 0 & L_{md} \end{bmatrix} \begin{bmatrix} i^r_{mq} \\ i^r_{md} \end{bmatrix}. \tag{2}$$

The Laplace operator is applied on the rotor voltage equations with short-circuited damper windings; the damper winding currents can be obtained

$$i'^r_{kqx} = -\frac{sL_{mq}i^r_{mq}}{r'_{kqx} + sL'_{lkqx}} \tag{3}$$

$$i'^r_{kdy} = -\frac{sL_{md}i^r_{md}}{r'_{kdy} + sL'_{lkdy}} \tag{4}$$

$$i'^r_{fd} = \frac{v'^r_{fd}}{r'_{fd} + sL'_{lfd}} - \frac{sL_{md}i^r_{md}}{r'_{fd} + sL'_{lfd}}. \tag{5}$$

The current through magnetizing inductances can be obtained by Kirchhoff's current law (KCL)

$$i^r_{mq} = \frac{i^r_{qs}}{\sum_{x=1}^{3}[-sL_{mq}/(r'_{kqx} + sL'_{lkqx})] - 1} \tag{6}$$

$$i^r_{md} = \frac{i^r_{ds} - [v'^r_{fd}/(r'_{fd} + sL'_{lfd})]}{\sum_{y=1}^{2}[-sL_{md}/(r'_{kdy} + sL'_{lkdy})] - 1 - [sL_{md}/(r'_{fd} + sL'_{lfd})]}. \tag{7}$$

Substituting (6) and (7) into the Laplace equation of stator voltage yields the relationship between stator voltages and stator currents, as shown (8) and (9) at the bottom of this page, where Z_{qq}, Z_{qd}, Z_{dq}, and Z_{dd} in the equation will be explained later.

$$v^r_{qs} = (Z_{qq})i^r_{qs} + (Z_{qd})i^r_{ds} - \omega_r L_{md}\frac{v'^r_{fd}/(r'_{fd} + sL'_{lfd})}{\sum_{y=1}^{2}[-sL_{md}/(r'_{kdy} + sL'_{lkdy})] - 1 - [sL_{md}/(r'_{fd} + sL'_{lfd})]} \tag{8}$$

$$v^r_{ds} = (Z_{dq})i^r_{qs} + (Z_{dd})i^r_{ds} - sL_{md}\frac{v'^r_{fd}/(r'_{fd} + sL'_{lfd})}{\sum_{y=1}^{2}[-sL_{md}/(r'_{kdy} + sL'_{lkdy})] - 1 - [sL_{md}/(r'_{fd} + sL'_{lfd})]} \tag{9}$$

The small-signal impedances on source side are related to the voltages and currents variations around steady state in the rotor reference frame by

$$\begin{bmatrix} \Delta V_{qs} \\ \Delta V_{ds} \end{bmatrix} = \begin{bmatrix} Z_{qq} & Z_{qd} \\ Z_{dq} & Z_{dd} \end{bmatrix} \begin{bmatrix} \Delta I_{qs} \\ \Delta I_{ds} \end{bmatrix} \tag{10}$$

where Δ denotes the small deviation of the respective variable from the equilibrium point. At any frequency of interest, $\Delta V_{qs}, \Delta V_{ds}, \Delta I_{qs}$, and ΔI_{ds} could be extracted from d–q quantities by fast Fourier transform (FFT) procedure.

By defining

$$A_q = \frac{L_{mq}}{\sum_{x=1}^{3} [-sL_{mq}/(r'_{kqx} + sL'_{lkqx})] - 1} \tag{11}$$

$$A_d = \frac{L_{md}}{\sum_{y=1}^{2} [-sL_{md}/(r'_{kdy} + sL'_{lkdy})] - 1 - [sL_{md}/(r'_{fd} + sL'_{lfd})]} \tag{12}$$

the d–q impedances can be expressed from (8) and (9) by

$$Z_{qq} = \frac{\Delta V_{qs}}{\Delta I_{qs}} = -r_s - sL_{ls} + sA_q \tag{13}$$

$$Z_{qd} = \frac{\Delta V_{qs}}{\Delta I_{ds}} = -\omega_r L_{ls} + \omega_r A_d \tag{14}$$

$$Z_{dq} = \frac{\Delta V_{ds}}{\Delta I_{qs}} = \omega_r L_{ls} - \omega_r A_q \tag{15}$$

$$Z_{dd} = \frac{\Delta V_{ds}}{\Delta I_{ds}} = -r_s - sL_{ls} + sA_d. \tag{16}$$

The previous equations describe the d–q impedance characteristics of the synchronous machine. However, if r_s is assumed to be known that can be easily obtained from the manufacturer or by straightforward measurement, then Z_{dq} and Z_{dd} can be determined directly from Z_{qq} and Z_{qd}. Therefore, in order to estimate the parameters, only Z_{qq} and Z_{qd} are needed, since they are linearly dependent on Z_{dq} and Z_{dd}. The four terms in the d–q impedance matrix are easily calculated by

$$Z_{qq} = \frac{\Delta V_{qs}(s/\omega_r) - \Delta V_{ds} - r_s \Delta I_{qs}(\omega_r/s) - r_s \Delta I_{ds}}{\Delta I_{qs}((\omega_r/s) + (s/\omega_r))} \tag{17}$$

$$Z_{qd} = \frac{\Delta V_{qs}(\omega_r/s) + \Delta V_{ds} + r_s \Delta I_{qs}(\omega_r/s) + r_s \Delta I_{ds}}{\Delta I_{ds}((\omega_r/s) + (s/\omega_r))} \tag{18}$$

$$Z_{dq} = -\frac{(Z_{qq} + r_s)\omega_r}{s} \tag{19}$$

$$Z_{dd} = \frac{Z_{qd} s}{\omega_r} - r_s. \tag{20}$$

It is important to note that these equations do not show any limit of the number of damper windings, and x in the equations can be any number since this is a general mathematical model. Therefore, the method applied in this paper actually can be applied to any kind of model with any number of damper windings on the q-axis or d-axis.

III. Small-Signal Injection Technique

The synchronous machine impedances can be determined using series small-signal voltage disturbances or shunt current disturbances [12]–[15] injected between the machine and its load. In this paper, the current injection method was chosen. The injected current could be a set of three-phase modulated currents [12]–[14], or line-to-line modulated currents [15]. The latter method is used in this paper.

When the currents are injected, the resulting machine terminal voltage perturbations and armature current perturbations at the injected frequency can be used to specifically calculate the synchronous machine impedances [13]. The voltages and currents must be transformed to the d–q reference frame and their components at the extracted frequency of interest. For example, the synchronous machine impedance equation (10) can be rewritten in the form

$$Ax = B \tag{21}$$

where

$$B = \begin{bmatrix} \mathrm{Re}(\Delta V_q) \\ \mathrm{Re}(\Delta V_d) \\ \mathrm{Im}(\Delta V_q) \\ \mathrm{Im}(\Delta V_d) \end{bmatrix}, \qquad x = \begin{bmatrix} \mathrm{Re}(Z_{qq}) \\ \mathrm{Re}(Z_{qd}) \\ \mathrm{Re}(Z_{dq}) \\ \mathrm{Re}(Z_{dd}) \\ \mathrm{Im}(Z_{qq}) \\ \mathrm{Im}(Z_{qd}) \\ \mathrm{Im}(Z_{dq}) \\ \mathrm{Im}(Z_{dd}) \end{bmatrix}$$

and A is the matrix required to satisfy (21) but is not written out here due to space constraints.

For a three-phase system with no zero-sequence current, the impedance matrix consists of four complex unknowns Z_{qq}, Z_{qd}, Z_{dq}, and Z_{dd}. Therefore, at least two sets of measurements are needed in order to solve the linear system equations.

In a general form, two ac disturbance current sets can be injected as

$$i_{a1\mathrm{inj}} = 0 \tag{22}$$

$$i_{b1\mathrm{inj}} = -I_m \cos(\omega_s t + \omega_e t + \phi_1) \tag{23}$$

$$i_{c1\mathrm{inj}} = I_m \cos(\omega_s t + \omega_e t + \phi_1) \tag{24}$$

$$i_{a2\mathrm{inj}} = 0 \tag{25}$$

$$i_{b2\mathrm{inj}} = -I_m \cos(\omega_s t - \omega_e t + \phi_2) \tag{26}$$

$$i_{c2\mathrm{inj}} = I_m \cos(\omega_s t - \omega_e t + \phi_2) \tag{27}$$

where I_m is the desired current injection amplitude, ω_e is the synchronous radian frequency, and ω_s is the injection radian frequency that will be swept over a range of interest. ϕ_1 and ϕ_2 represent the injections having different initial angles. In *abc*, the injected currents include terms at frequencies $|\omega_s + \omega_e|$ and $|\omega_s - \omega_e|$. After transformation to a rotor reference frame, the

injected current in the d–q frame can be expressed as

$$i_{q1\mathrm{inj}} = \frac{1}{\sqrt{3}} I_m \sin(\omega_s t + \phi_1) - \frac{1}{\sqrt{3}} I_m \sin(\omega_s t + 2\omega_e t + \phi_1) \tag{28}$$

$$i_{d1\mathrm{inj}} = \frac{1}{\sqrt{3}} I_m \cos(\omega_s t + \phi_1) + \frac{1}{\sqrt{3}} I_m \cos(\omega_s t + 2\omega_e t + \phi_1) \tag{29}$$

$$i_{q2\mathrm{inj}} = -\frac{1}{\sqrt{3}} I_m \sin(\omega_s t + \phi_2) + \frac{1}{\sqrt{3}} I_m \sin(\omega_s t - 2\omega_e t + \phi_2) \tag{30}$$

$$i_{d2\mathrm{inj}} = \frac{1}{\sqrt{3}} I_m \cos(\omega_s t + \phi_2) + \frac{1}{\sqrt{3}} I_m \cos(\omega_s t - 2\omega_e t + \phi_2). \tag{31}$$

It can be seen that in the rotor reference frame, the injection currents contain components at frequencies ω_s and other terms. For impedance measurement, the terms at frequency ω_s are of interest, while the rest of the components can be ignored.

Using this method, the magnitude of q- and d-axis terms of injected current is maintained while the injected signals are symmetrical about the d-axis. It can be seen from (28)–(31) that the two injected vectors are both at frequency ω_s, but are rotating at opposite directions; therefore, they are not linearly dependent, and thus can be used to obtain the desired impedance. The solution represents a best fit to the data obtained from the current injection and can be automatically solved using a math processing software such as MATLAB. Using this method, to obtain an impedance value at one frequency point, two current injections are needed at two different frequencies. However, for the mathematical model described in (17)–(20), only two complex unknowns exist in two equations besides the armature resistance. That means only one measurement is necessary to obtain the synchronous machine d–q impedance matrix. Since the armature resistance is easy to find, this convenient property could be used to reduce the required measurement found with only current disturbance injected at one frequency.

IV. Online AC Impedance Measurement

The previous section described ideal currents that can be injected to determine the synchronous machine impedance. As a practical matter, this current injection can be accomplished by the line-to-line chopper circuit shown in Fig. 2.

The transistors are switched using a square-wave command with a fixed 50% duty cycle and a frequency set to $|\omega_s \pm 2\omega_e|$ [15]. For the study described later, the chopper circuit was operating with $R_c = 250\ \Omega$ and $C_c = 5\ \mu$F. The capacitor C_c used in this circuit is small in value and operates as a snubber to extinguish voltage spikes caused by switching and the inductive nature of the synchronous machine and connected load. Therefore, it does not significantly affect the impedance measurement.

At each frequency, the three phase voltages and currents of the synchronous machine are recorded and voltage and current d–q terms of rotor reference frame at the frequency of interest

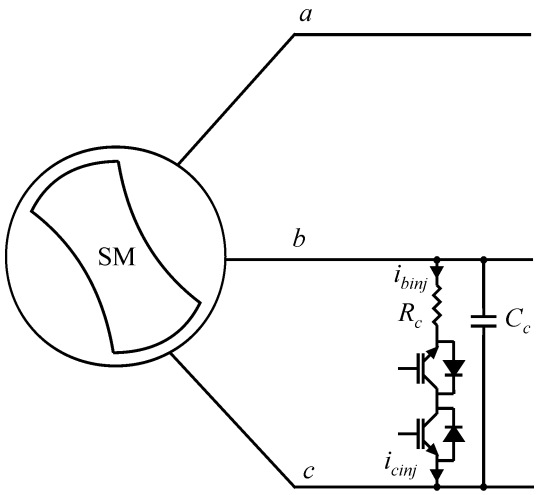

Fig. 2. Practical current injection technique.

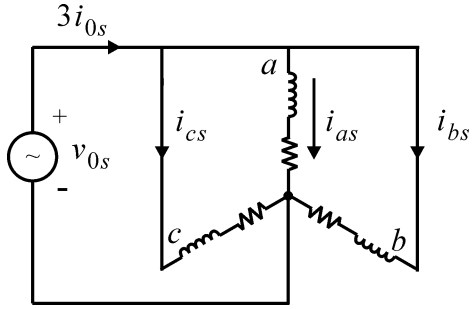

Fig. 3. Zero-sequence test circuit.

can be extracted by an FFT operation. The d–q impedance is then calculated from (10).

The primary advantage of the chopper circuit is that the switching frequency is set to be $|\omega_s \pm 2\omega_e|$. Compared with injection frequencies used a pulsewidth modulation (PWM) H-bridge converter [14], the injection frequencies in the proposed chopper circuit is much lower. Therefore, this circuit is more suitable for high-voltage and medium-voltage systems where transistor switching frequency is limited. The primary disadvantage is that the injected current will have considerable harmonics. However, it will not disturb normal system operation because the harmonics are much less than the fundamental injected current, which is typically selected to be less than 5% of rated machine current. Only quantities at the frequency of interest will be extracted. Also, the injection device has no limit on the working condition, so it could be used to extract the parameters of the machine in an operating condition with any different load level.

V. Parameter Identification

A. Identification of Stator Resistor and Inductance

In the proposed technique, r_s is assumed to be known, and it could be very easily obtained by a zero-sequence test [1]. The zero-sequence test circuit is shown in Fig. 3. The three-phase stator terminals are connected together; a sinusoidal voltage is

applied between the neutral point and connected points. The corresponding stator resistor and inductance can be obtained from

$$r_s + j\omega_e L_{ls} = \frac{v_{0s}}{i_{0s}}. \tag{32}$$

The dc resistance of the armature windings is very sensitive to variations in winding temperature [1]. To take the temperature dependency into account, the winding resistance is measured right after the injection test, before the windings cool down. Also, in the proposed method, the test period is rather short, and the machine temperature rise is not significant. Therefore, there are only slight variations in dc resistance. If even higher accuracy is required, the measured resistance value at one temperature can be corrected to the desired temperature by recording current temperature, specified temperature, test value of winding resistance, and characteristic constant of winding material [1].

B. Genetic Algorithm

Once the d–q synchronous machine impedance is obtained, the optimal set of solution of machine parameters can be identified using a GA by minimizing the error between the mathematical models (13)–(16), (17)–(20), and the experimental data.

The GA was developed from the Darwinian evolution theory of "survival of the fittest." This technique was selected in this paper because it does not require an initial estimation, and also the objective function is very simple in which only the fitness values based on the objective functions are used [16]. GAs have a lot of applications with good results in many practical problems and have been shown to be a powerful tool to solve optimization problems such as identification of machine parameters [17]–[20]. In this paper, a MATLAB-based toolbox Genetic Optimization System Engineering Tool (GOSET) [16] is used to implement the GA.

In practical applications, each parameter is codified into a gene. The parameters that need to be identified for synchronous machine model is the vector $[r_s, L_{ls}, L_{mq}, r'_{kq1}, L'_{kq1}, r'_{kq2}, L'_{kq2}, r'_{kq3}, L'_{kq3}, L_{md}, r'_{kd1}, L'_{kd1}, r'_{kd2}, L'_{kd2}, r'_{fd}, L'_{fd}]$. r_s and L_{ls} could be removed if they are already obtained by the zero-sequence test. And the fitness function is obtained by the error between test impedance and estimated impedance

$$F = \frac{1}{\varepsilon + (1/N)\sqrt{\sum_{k=1}^{N} |Z_{xy\_\mathrm{meas}_k} - Z_{xy\_GA_k}|/|Z_{xy\_\mathrm{meas}_k}|}} \tag{33}$$

where N is the number of measured frequencies, $Z_{xy\_\mathrm{meas}_k}$ is the tested result, Z_{qq}, Z_{qd}, Z_{dq}, and Z_{dd}, by the injection method, $Z_{xy\_GA_k}$ is the estimated value from the GA, and ε is a very small value to avoid an infinite fitness function.

VI. Simulation and Laboratory Validation

In the simulated system, the generator was connected to an RL load with values of $R = 14.42\ \Omega$ and $L = 1.09$ mH. The generator is a salient-pole machine rated at 3.7 kW, 230 V, with four-poles and a rated speed of 1800 r/min. Fig. 4 shows the diagram for the simulation setup as simulated in the Advanced Continuous Simulation Language (ACSL) [21]. The machine

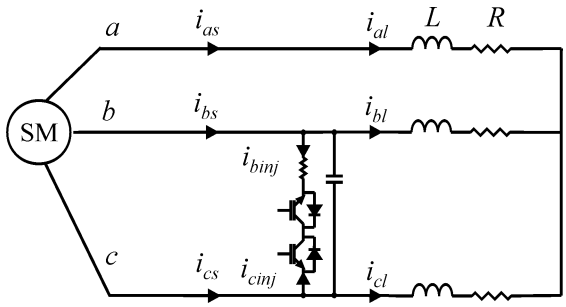

Fig. 4. System used for validation.

parameters in the model were originally obtained by performing a series of synchronous measurements and SSFR tests on a laboratory machine. The injection current was 5% of the rated armature current and was swept over a frequency range of 0.01–1000 Hz and synchronous machine impedance was extracted for each frequency. For the study described later, the chopper circuit was operating with $R_c = 250\ \Omega$ and $C_c = 5\ \mu$F.

A. Double-Frequency-Sweep Injection and Single-Frequency-Sweep Injection Comparison in Simulation

A Jacobian analysis was applied to the synchronous machine model in ACSL to obtain the Thevinin d–q impedance matrix [21]. This is a frequency-domain calculation about the operating point by numerical perturbation. The Jacobian d–q impedance matrix was used to compare estimated results as the reference [14], [15].

Since the impedance matrix consists of four complex unknowns and two axis equations are available, a second set of linear independent injection is needed to solve the impedance matrix. This is called double-frequency-sweep injection herein and is generally necessary for impedance measurement in three-phase ac systems [14], [15]. Fig. 5 shows the magnitude and phase of the d–q impedances identified with the double-frequency-sweep injection method. The impedance values were processed with the GA algorithm, and a set of synchronous machine parameters was extracted. Based on the extracted machine parameters, the impedances were calculated using (13)–(16) and plotted in Fig. 5. It can be seen that the impedance curves are very close to those obtained from Jacobian analysis.

Because the stator resistance of most synchronous machines can be measured directly in advance, four complex unknowns in the impedance matrix could be decreased to two complex unknowns. With two axis equations available, only one frequency sweep is needed to identify the impedance and machine parameter for this specific impedance measurement. This is a great advantage for such application because of the reduced amount of measurements. The results with the single frequency sweep from 0.3 to 1000 Hz are also plotted in the Fig. 5 and are seen to be very similar to the results of the double-frequency-sweep injection results.

It is worth noting the sensitivity of the proposed technique when the injection frequency is close to the synchronous frequency. Equations (17)–(20) show that the denominator of Z_{qq}

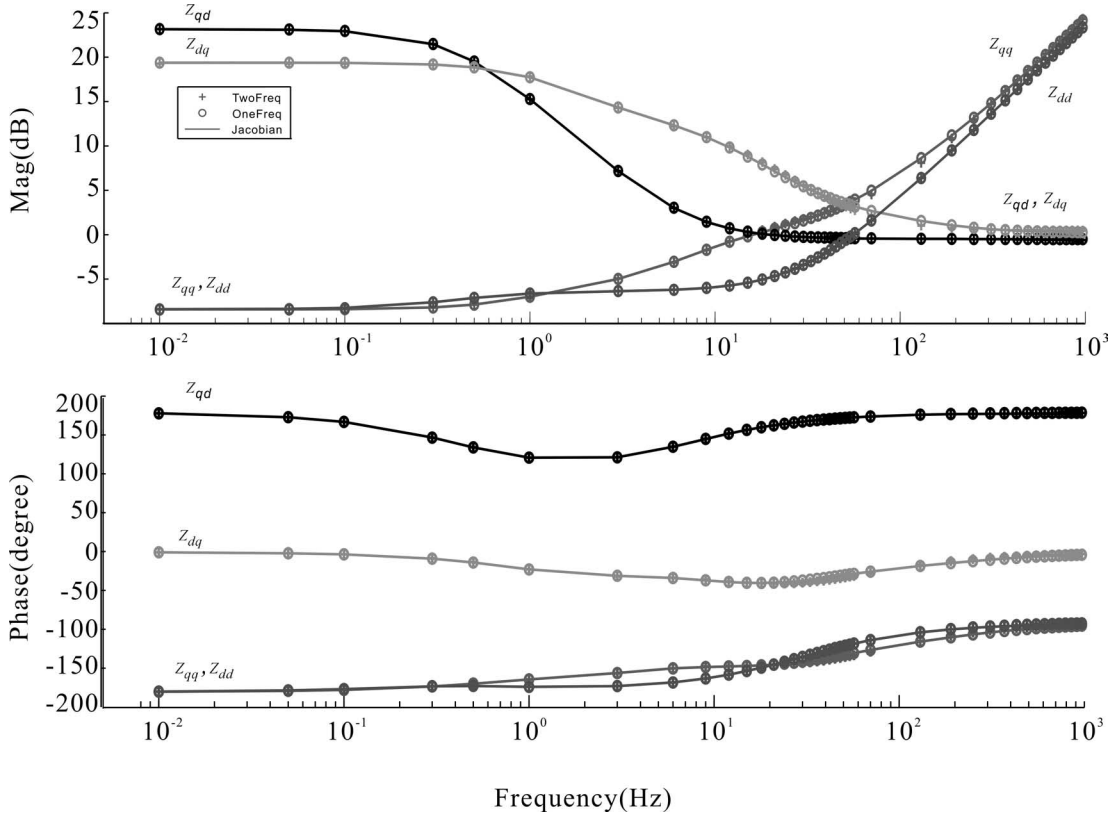

Fig. 5. Magnitude and phase of d–q impedance by single-frequency-sweep and double-frequency-sweep injection.

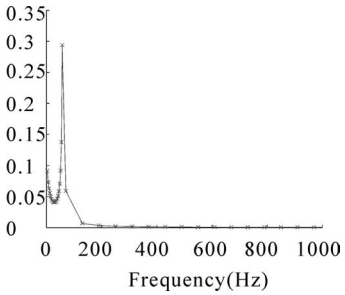

Fig. 6. Sensitivity of Z_{qq} to injected frequency.

and Z_{qd} will approach zero when the injection frequency approaches ω_e, and this means the sensitivity of impedance will be high around ω_e. Fig. 6 is a plot of the sensitivity of Z_{qq}. In practical test, the measurements around ω_e should be avoided and the values at these points can be obtained by a curve-fitting procedure. Also to avoid the effects of system harmonics on the injection signal measurement, all the frequencies that are multiples of system fundamental frequency were avoided during the test.

B. Laboratory Verification

In the laboratory, the system of Fig. 4 was constructed. The injection circuit was applied at the terminal of the synchronous machine. However, the mathematical models (13)–(16) and (17)–(20) are based on the rotor reference frame. Therefore, a position encoder was used in order to obtain the position angle of the rotor reference frame.

As shown in the previous section, the single-frequency-sweep injection can obtain almost the same results as the double-frequency-sweep injection. So, the single-frequency-sweep injection with frequencies from 0.3 to 1000 Hz was applied in the laboratory. Fig. 7 shows the waveforms of a-phase and b-phase currents. During the injection process, the wave shape of b-phase currents has a little change due to the small-signal injection. Since the current injection is small, it will not affect the normal operating condition. The rotor speed shows pretty good constant characteristic before and during injection. The speed was obtained with a dc tachometer, and therefore shows ripple due only to the tachometer commutation.

The value of r_s was obtained by the zero-sequence test. The other parameters were estimated by the GA as shown in Table I. Another set of parameters was obtained from the synchronous measurements, and SSFR tests are used for comparison. The small-signal impedances are compared in the frequency domain in Fig. 8. The frequency points around ω_e are avoided in the laboratory test and are added in Fig. 8 based on the trend of the curve. The solid line represents the Jacobian impedance from the simulation based on the parameters obtained from the frequency response test. The cross marks represent the direct laboratory measurement impedance results using line-to-line injection technique. The laboratory measured impedance curves are used to estimate the real machine parameters by the GA that are shown in the Table I. The impedance curve obtained by

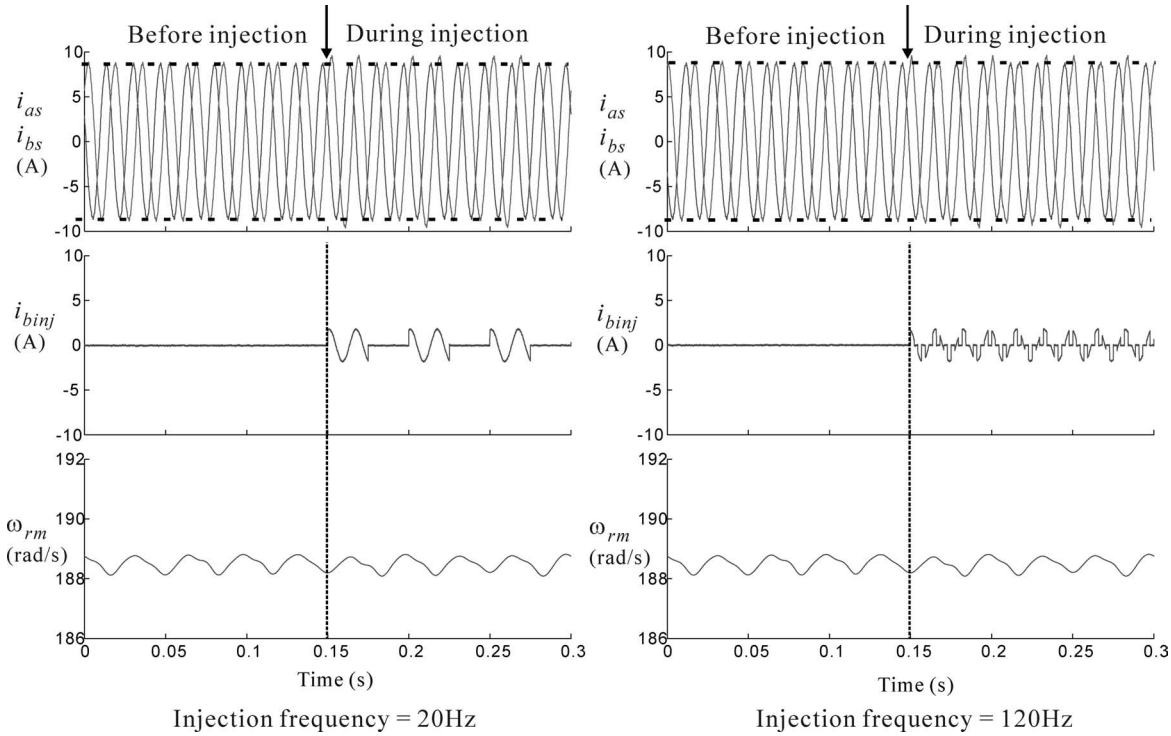

Fig. 7. Waveforms of phase currents, injected current, and rotor speed for two different injection frequencies.

TABLE I
EXTRACTED SYNCHRONOUS MACHINE PARAMETERS

L_{ls}	2.03mH	r_s	0.382 Ω
L_{mq}	25.3mH	L_{md}	37.9mH
r'_{kq1}	5.96 Ω	r'_{fd}	0.115 Ω
L'_{kq1}	39.2nH	L'_{fd}	0.7852mH
r'_{kq2}	1.88 Ω	r'_{kd1}	1.607 Ω
L'_{kq2}	1.09mH	L'_{kd1}	27.6nH
r'_{kq3}	0.507 Ω	r'_{kd2}	2.54 Ω
L'_{kq3}	5.597mH	L'_{kd2}	0.87mH

(17)–(20) is called laboratory GA impedance, and is represented by the circle symbol. As can be seen, with both of extracted parameters and original parameters, the d–q impedance plots matched closely, which means the transient characteristics and performance of the synchronous machine can be predicted accurately. Some main parameters such as stator inductor and magnetizing inductances that are necessary for the steady-state analysis are listed in the Table II to have a comparison between the proposed method and original SSFR method. The q-axis and d-axis operational impedances are used for studying machine electrical characteristic [16], which is defined as

$$X_q(s) = -\frac{\psi^r_{qs}}{i^r_{qs}} \tag{34}$$

$$X_d(s) = -\left.\frac{\psi^r_{ds}}{i^r_{ds}}\right|_{v'_{fd}=0} \tag{35}$$

and the operational impedances are also plotted in the Fig. 9 for comparison. As can be seen, the characteristics obtained with the proposed method compare well to those obtained using the SSFR method. A slight discrepancy exists between the stator leakage inductance values using the SSFR and the proposed method. In this case, stator leakage inductance obtained from the zero-sequence test might be more accurate. The online

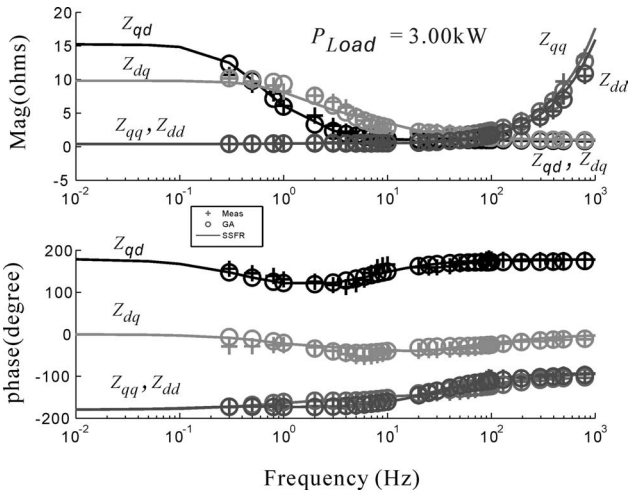

Fig. 8. Comparison of d–q impedance from SSFR parameters and parameters extracted using the proposed technique.

TABLE II
COMPARISON OF MAIN PARAMETERS

	SSFR parameters	Extracted parameters
L_{ls}	1.12 mH	2.03mH
L_{mq}	24.9 mH	25.3mH
L_{md}	39.3 mH	37.9mH
r'_{fd}	0.11 Ω	0.115 Ω

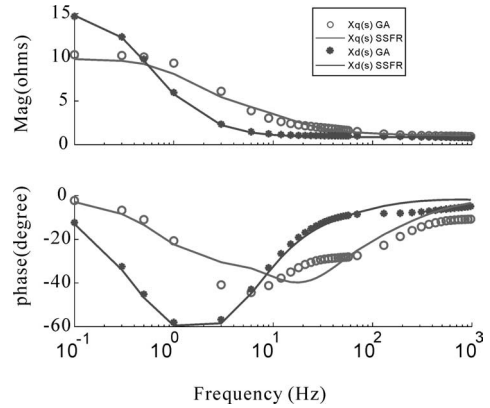

Fig. 9. Operational impedance comparison.

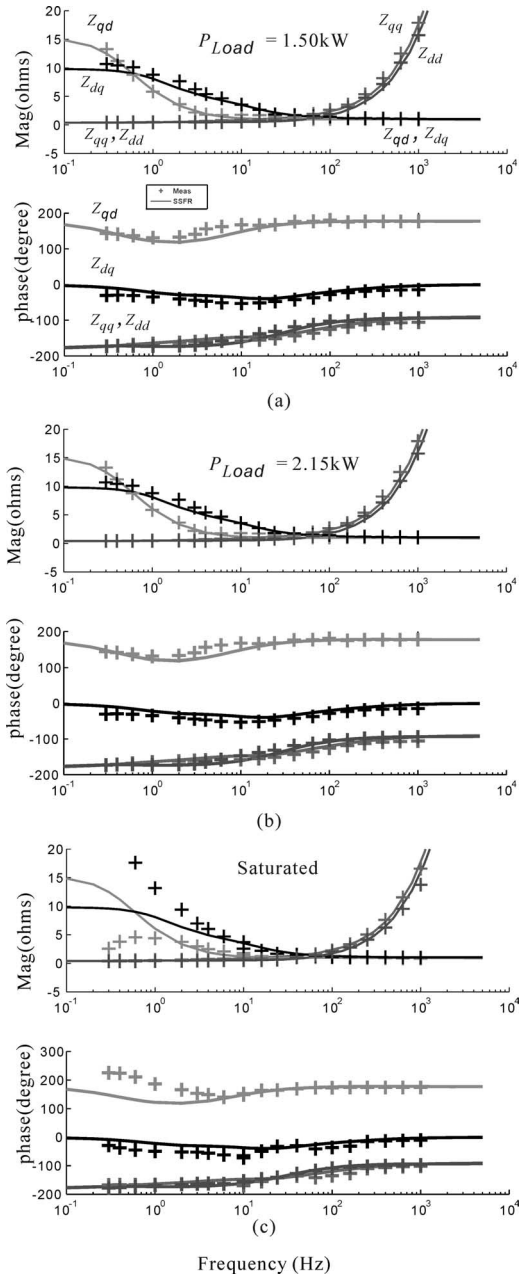

Fig. 10. Comparison at various load levels.

identification method yields a different value because several other parameters are being determined at the same time. However, since the stator leakage inductance could be very easily obtained by a zero-sequence test, the parameters from the proposed method could be used with the leakage inductance from the zero-sequence test in the model.

The previous test has a 3.0-kW load with 0.53 A filed current applied to the excitation. Different load levels (1.50 kW with 0.36 A field current, 2.15 kW with 0.45 A field current, 4.65 kW with 1.2 A field current) are tested, and the SSFR and measured small-signal impedance are plotted in Fig. 10. As can be seen, when the machine is not saturated, the measured results are similar. When the machine is saturated, the measured impedance curve changes and the extracted parameters are also changed due to the saturation.

VII. Conclusion

This paper introduced a new method of performing online parameter measurement of synchronous machines. The method is based on a simple chopper circuit that is connected between two phases of the machine to create voltage and current disturbances. Using this circuit and a mathematical model of the synchronous machine, all of the necessary machine parameters can be determined. This provides an alternative to other machine tests, such as SSFR, short circuit, and load rejection. The new method was validated using laboratory measurements on a 3.7-kW synchronous machine.

Appendix A

The switching waveform for the chopper transistor command is a square wave that can be expressed by the sum of a series of the harmonics of the switching frequency

$$sw = d + 2\sum_{k=1}^{\infty} \frac{\sin(k\pi d)}{k\pi} \cos(k\omega t) \tag{36}$$

where d is the duty cycle, k is the harmonic number, and ω is the switching frequency, which was $|\omega_s \pm 2\omega_e|$.

The coefficient of each harmonic is $2\sin(k\pi d)/k\pi$ with an offset of d; the value of which will decrease as k increases. It can be seen the term at the switching frequency is dominant. When the duty cycle d is set to 50%, this term will have maximum amplitude.

The equivalent admittance of the chopper circuit in Fig. 2 is

$$Y = \frac{sw}{R_c}. \tag{37}$$

Considering the dominant terms of the waveform, the injected currents at $|\omega_s + 2\omega_e|$ and $|\omega_s - 2\omega_e|$ become

$$\begin{aligned} i_{\text{binj}} = v_{bc}Y &= \frac{V_{ll}\cos(\omega_e t + \phi)}{R_c}\left(\frac{1}{2} + \frac{2}{\pi}\cos(\omega_s t + 2\omega_e t)\right) \\ &= \frac{V_{ll}}{2R_c}\cos(\omega_e t + \phi) + \frac{V_{ll}}{\pi R_c}\cos(\omega_s t + 3\omega_e t + \phi) \\ &\quad + \frac{V_{ll}}{\pi R_c}\cos(\omega_s t + \omega_e t - \phi) \end{aligned} \tag{38}$$

and

$$i_{b\text{inj}} = v_{bc}Y = \frac{V_{ll}\cos(\omega_e t+\phi)}{R_c}\left(\frac{1}{2}+\frac{2}{\pi}\cos(\omega_s t-2\omega_e t)\right)$$
$$= \frac{V_{ll}}{2R_c}\cos(\omega_e t+\phi)+\frac{V_{ll}}{\pi R_c}\cos(\omega_s t-3\omega_e t-\phi)$$
$$+\frac{V_{ll}}{\pi R_c}\cos(\omega_s t-\omega_e t+\phi) \quad (39)$$

where d is set to be 0.5 and ϕ is the phase difference between the three-phase line-to-line voltage v_{bc} and the square-wave signals. The last terms of (38) and (39) are exactly the desired injection current defined in (22)–(27). Although the expression of (38) and (39) has more terms than needed, these terms will be mathematically removed by the FFT technique during data processing.

Therefore, the chopper circuit, switching at a frequency of $|\omega_s \pm 2\omega_e|$, produces three-phase injection currents that contain components at frequencies $|\omega_s \pm \omega_e|$. These components become the desired ω_s terms when transformed into the rotor reference frame.

ACKNOWLEDGMENT

This work was sponsored by Naval Sea Systems Command under contract N00024-05-MR-66021.

REFERENCES

[1] *IEEE Guide: Test Procedures for Synchronous Machine*, IEEE Standard 115 A, 1983.
[2] F. P. de Mello and J. R. Ribeiro, "Derivation of synchronous machine parameters from tests," *IEEE Trans. Power App. Syst.*, vol. PAS-96, no. 4, pp. 1211–1218, Jul./Aug. 1977.
[3] E. da Costa Bortoni and J. A. Jardini, "Identification of synchronous machine parameters using load rejection test data," *IEEE Trans. Energy Convers.*, vol. 17, no. 2, pp. 242–247, Jun. 2002.
[4] H. Tsai, J. Demcko, and R. G. Farmer, "On-line synchronous machine parameter estimation from small disturbance operating data," *IEEE Trans. Energy Convers.*, vol. 10, no. 1, pp. 25–36, Mar. 1995.
[5] H. B. Karayaka, A. Keyhani, B. L. Agrawal, D. A. Selin, and G. T. Heydt, "Identification of armature, field, and saturated parameters of a large steam turbine-generator from operating data," *IEEE Trans. Energy Convers.*, vol. 15, no. 2, pp. 181–187, Jun. 2002.
[6] H. B. Karayaka, A. Keyhani, G. T. Heydt, B. Agrawal, and D. Selin, "Neural network based modeling of a large steam turbine-generator rotor body parameters from on-line disturbance data," *IEEE Trans. Energy Convers.*, vol. 16, no. 4, pp. 305–311, Dec. 2001.
[7] H. B. Karayaka, A. Keyhani, G. T. Heydt, B. L. Agrawal, and D. A. Selin, "Synchronous generator model identification and parameter estimation from operating data," *IEEE Trans. Energy Convers.*, vol. 18, no. 1, pp. 121–126, Mar. 2003.
[8] E. Kyriakides, G. T. Heydt, and V. Vittal, "Online parameter estimation of round rotor synchronous generators including magnetic saturation," *IEEE Trans. Energy Convers.*, vol. 20, no. 3, pp. 529–537, Sep. 2003.
[9] F. P. de Mello and L. N. Hannett, "Determination of synchronous machine electrical characteristics by test," *IEEE Trans. Power App. Syst.*, vol. 102, no. 12, pp. 3810–3815, Dec. 1983.
[10] *IEEE Guide for Synchronous Generator Modeling Practices in Stability Analyses*, IEEE Standard 1110, 1991.
[11] P. C. Krause, O. Wasynczuk, and S. D. Sudhoff, *Analysis of Electric Machinery and Drive Systems*. Piscataway, NJ: IEEE Press, 2002.
[12] M. Belkhayat, "Stability criteria for AC power systems with regulated loads," Ph.D. dissertation, Purdue Univ, West Lafayette, IN, Dec. 1997.
[13] M. Belkhayat and M. L. Williams, "Impedance extraction techniques for DC and AC systems," presented at the Naval Symp. Electr. Mach., Philadelphia, PA, Dec. 2000.
[14] Y. L. Familiant, K. A. Corzine, J. Huang, and M. Belkhayat, "AC impedance measurement techniques," in *Proc. IEEE Electr. Mach. Drive Conf.*, San Antonio,, TX, May 2005, pp. 1850–1857.
[15] J. Huang and K. A. Corzine, "AC impedance measurement by line-to-line injected current," in *Proc. IEEE Ind. Appl. Soc. Conf.*, Tampa, FL, Oct. 2006, vol. 1, pp. 300–306.
[16] C. Kwon and S. D. Sudhoff, "A genetic algorithm based induction machine characterization procedure," in *Proc. IEEE Int. Conf. Electr. Mach. Drives*, May 15, 2005, pp. 1358–1364.
[17] K. S. Huang, W. Kent, Q. H. Wu, and D. R. Turner, "Parameter identification of an induction machine using genetic algorithms," in *Proc. IEEE Int. Symp. Comput.-Aided Control Syst. Des.*, 1999, vol. 1, pp. 510–515.
[18] F. Alonge, F. D'Ippolito, G. Ferrante, and F. M. Raimondi, "Parameter identification of induction motor model using genetic algorithms," in *Proc. IEEE Control Theory Appl. Conf.*, Nov. 1998, vol. 145, no. 6, pp. 587–593.
[19] H. Razik, C. Defranoux, and A. Rezzoug, "Identification of induction motor using a genetic algorithm and a quasi-Newton algorithm," in *Proc. IEEE Power Electron. Congr.*, Oct. 2000, pp. 65–70.
[20] R. Escarela-Perez, T. Niewierowicz, and E. Campero-Littlewood, "Synchronous machine parameters from frequency-response finite-element simulations and genetic algorithms," *IEEE Trans. Energy Convers.*, vol. 16, no. 2, pp. 198–203, Jun. 2001.
[21] *Advanced Continuous Simulation Language Reference Manual*, version 11, MGA Softw., Concord, MA, 1995.

Jing Huang (S'04) received the B.S.E.E. degree from Nan Chang University, Nan Chang, China, in 1997, the M.S.E.E. degree from the North China Electrical Power University, Beijing, China, in 2000, and the M.S.E.E. degree from the University of Missouri, Rolla, in 2005. She is currently working toward the Ph.D. degree at Missouri University of Science and Technology, Rolla.

From 2000 to 2003, she was with Beijing Sifang Automation Company, Ltd. Her current research interests include power electronics, multilevel converters, electrical machinery, and motor controls.

Keith A. Corzine (S'92–M'97–SM'06) received the B.S.E.E., M.S.E.E., and Ph.D. degrees from the University of Missouri, Rolla, in 1992, 1994, and 1997, respectively.

From 1997 to 2004, he was with the University of Wisconsin, Milwaukee. He is currently a Professor at Missouri University of Science and Technology, Rolla. His current research interests include power electronics, motor drives, naval ship propulsion system, and electric machinery analysis.

Mohamed Belkhayat received the Ph.D. degree in electrical engineering from Purdue University, West Lafayette, IN.

He was with the Naval Postgraduate School and the Naval Academy. He is currently a Research Engineer at Northrop Grumman, Washington, DC. His current research interests include modeling, simulation, and analysis of advanced naval power systems.